Electronic Supplementary Information

Morphology Control towards Greener, Non-halogenated Solvent System Processed $CH_3NH_3PbI_3$ Film for High Performance Perovskite Solar Cells

Wan-Yi Tan, Peng-Peng Cheng, Yong-Wen Zhang, Jia-Ming Liang, Xudong Chen, Yidong Liu, and Yong Min**

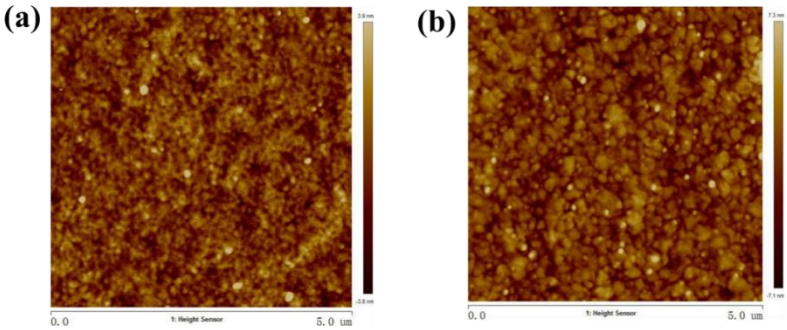

Figure S1 Topographic atomic force microscopy (AFM) images (5 μm × 5 μm) of (a) the p-perovskite film, R_{rms} = 1.15 nm, and (b) m-perovskite film, R_{rms} = 2.04 nm. Both of the thin-films were deposited on ITO/NiO_x substrates.

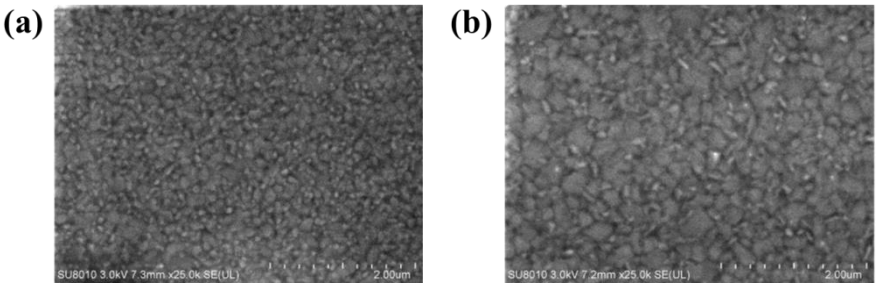

Figure S2 SEM images of (a) the p-perovskite film and (b) m-perovskite film. Both of the thin-films were deposited on ITO/NiO_x substrates and covered with $PC_{61}BM$ layer.

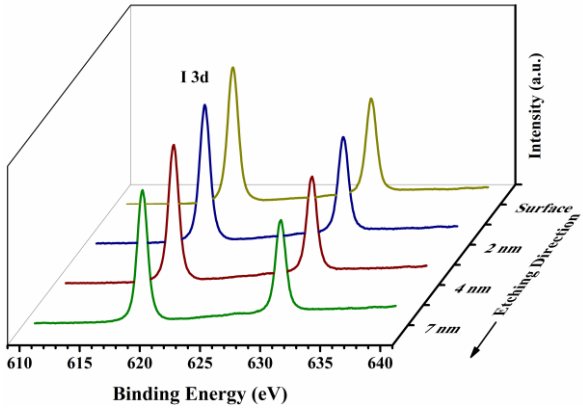

Figure S3 XPS depth profiling of I component in m-perovskite film.

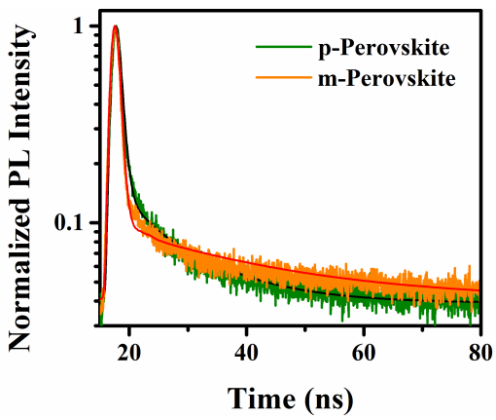

Figure S4 Normalized transient PL decay profiles of the p-perovskite film and m-perovskite film measured at 780 nm, from the air side.

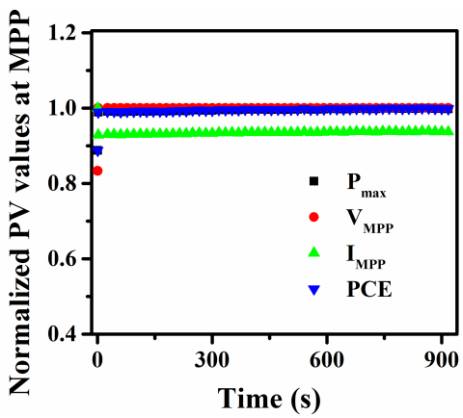

Figure S5 Stabilized power output of m-PSC, obtained at a maximum power point (MPP).

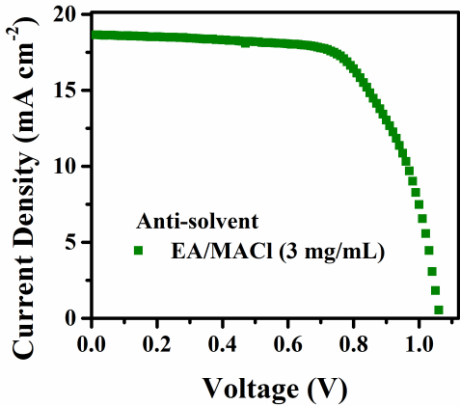

Figure S6 Current density (*J*)–voltage (*V*) characteristics of the reverse swept $MAPbI_3$ PSC with the perovskite layer using EA/MACl (3 mg/mL) as the anti-solvent.

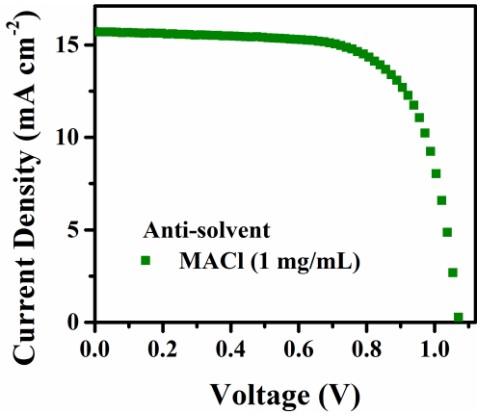

Figure S7 Current density (*J*)–voltage (*V*) characteristics of the reverse swept $MAPbI_3$ PSC with the perovskite layer only modified by MACl.

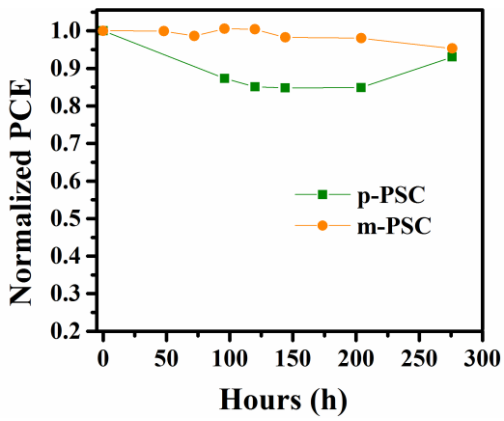

Figure S8 Stability of PSCs based on p-perovskite and m-perovskite films, which stored in ambient air at ~53% humidity in the dark.

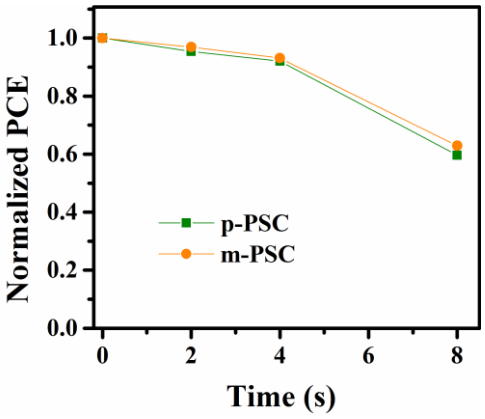

Figure S9 Stability of PSCs based on p-perovskite and m-perovskite films, which thermally annealed at 85 ℃.

Table S1 Comparison of the PCE of NMP-processed PSCs reported in this work and in the literatures.

Precursor solvent	**Anti-solvent**	**Device configuration**	**Thermal annealing condition**	**PCE**	**Ref.**
NMP	Dipping in ether for 30 min	FTO/c-TiO_2/TiO_2/$MAPbI_3$/Al_2O_3/Carbon	Room-temperature annealing for over 100 h	12.3%	1
NMP	None	FTO/c-TiO_2/TiO_2/$MAPbI_3$/ Al_2O_3/Carbon	Slow crystallization for 120 h	15.0%	2
GBL:DMSO :NMP (2:2:1)	CB	ITO/PEDOT:PSS/$MAPbI_3$/ PCBM/LiF/Al	Thermally annealed at 85 ^{o}C for 1 h	12.3%	3
DMAc/NMP (4:1)	Toluene	FTO/compact TiO2/mesoporous TiO_2/$MAPbI_3$/spiro-OMeTAD/Au	Annealing free	17.09%	4
DMF/DMSO/ NMP (4:1:0.25)	CB	FTO/TiO_2/ $Cs_{0.05}(MA_{0.17}FA_{0.83})_{0.95}Pb(I_{0.83}Br_{0.17})_3$/ spiro-OMe-TAD/Au	Thermally annealed at 100 ^{o}C for 1 h	19.61%	5
DMAc/NMP (5:1)	Toluene	FTO/TiO_2/$MAPbI_3$/spiro-OMeTAD/Ag	Thermally annealed at 105 ^{o}C for 10 min	15.25%	6

Table S2 Time resolved photoluminescence characterization of the p-perovskite film and m-perovskite film on ITO/NiO_x substrates.

Active layer	τ_1 (ns)	Fraction 1	τ_2 (ns)	Fraction 2
p-Perovskite	0.7	61.79%	11.9	38.21%
m-Perovskite	0.55	56.52%	25.5	43.48%

Table S3 The photovoltaic performance of the reverse swept $MAPbI_3$ PSCs with the perovskite layer using different anti-solvents.

Anti-solvent	**PCE (%)**	**J_{SC} (mA cm^{-2})**	**V_{OC} (V)**	***FF* (%)**	**R_s (Ω cm^2)**	**R_{sh} (kΩ cm^2)**
EA/MACl (3 mg/mL)	13.16	18.65	1.06	66.55	4.44	1.48
MACl (1 mg/mL)	11.71	15.70	1.07	69.66	4.21	1.57

Reference

1 C. Y. Chan, Y. Y. Wang, G. W. Wu, E. W. G. Diau, *J. Mater. Chem. A*, 2016, **4**, 3872–3878.

2 C. M. Tsai, G. W. Wu, S. Narra, H. M. Chang, N. Mohanta, H. P. Wu, C. L. Wang, E. W. G. Diau, *J. Mater. Chem. A*, 2017, **5**, 739–747.

3 L. Xie, H. Hwang, M. Kim, K. Kim, *Phys. Chem. Chem. Phys*., 2017, **19**, 1143−1150.

4 X. Fang, Y. H. Wu, Y. T. Lu, Y. Sun, S. Zhang, J. Zhang, W. H. Zhang, N. Y. Yuan, J. N. Ding, *J. Mater. Chem. C*, 2017, **5**, 842−847.

5 T. Y. Wu, J. H. Wu, Y. G. Tu, X. He, Z. Lan, M. L. Huang, J. M. Lin, *J. Power Sources*, 2017, **365**, 1−6.

6 M. H. Lv, W. Lv, X. Fang, P. Sun, B. C. Lin, S. Zhang, *RSC Adv.*, 2016, **6**, 35044–35050.